Global Flow Measurement Workshop
22 - 24 October 2024

Technical Paper

Quantifying Uncertainty in Offshore Flare Emission Calculations: A Comprehensive Analysis

Phil Stockton, Accord ESL

1 INTRODUCTION

Accord developed their Combustor software tool to calculate methane, CO2 and CO2e[1] emissions from offshore flares. Combustor calculates flare combustion efficiency (CE) using a semi-empirical equation developed by the University of Alberta (UoA) [1], which is included in the Oil and Gas methane Partnership (OGMP) 2.0 technical guidance [2].

According to the ISO Guide to the Expression of Uncertainty in Measurement (GUM) [3], reporting of an uncertainty associated with the measurement of any physical quantity is obligatory. Hence, it is necessary to provide uncertainties for the calculated combustion efficiency and associated methane and CO2e emissions produced by Combustor.

The paper builds on work presented in a previous paper, entitled “Offshore flares: measurement and calculation of combustion efficiency, methane and CO2e emissions” [4], and presents a comprehensive analysis of uncertainty of offshore flare emission calculations using the UoA equation.

We investigate the various sources of uncertainty, including input measurements (e.g. flare flow rate, flare gas lower heating value (LHV), wind tunnel gas speed, etc.) as well as uncertainties stemming from the mathematical formulation of the UoA equation itself.

The paper begins by summarising the advantages of the closed loop wind tunnel, used to develop the UoA equation, in providing robust data to calculate efficiency with low measurement uncertainty. This also allowed an analysis of the goodness of fit of the form of the combustion efficiency equation itself to be assessed. The uncertainty in the model is encapsulated in the uncertainty in the coefficients of the fitted equation. This uncertainty determination also includes the covariance between the coefficients.

The uncertainty analysis is extended to Combustor measurements in the field using real data from the measurement of wind speed, flare exit velocity, etc., whose uncertainties also contribute to the ‘live’ combustion efficiency and CO2e emission calculations.

A key component of Combustor is the CHARM process simulation model, which is used to calculate the flare composition and its Lower Heating Value (LHV). The paper explains the method used to determine the uncertainty in the CHARM modelled flare properties and process simulations more generally. Comparisons with real sampled compositions are presented. The advantages of using process simulations to predict the flare composition and properties are also highlighted.

We demonstrate the influence of varying input conditions on the predicted combustion efficiency and quantify the resulting uncertainty distributions. The analysis is then extended to the CO2e emissions.

[1] Carbon dioxide equivalent (CO2e) is a unit of measurement that compares the global warming potential (GWP) of different greenhouse gases (GHGs). It's used to express the amount of carbon dioxide (CO2) that would have the same global warming impact as a given amount of another GHG.

The term flare gas has been used to refer to the gas that is routed to the flare stack and tip prior to combustion. The gases emanating from the flare after combustion are referred to as the flare plume.

2 Uncertainty in Measuring Combustion Efficiency

2.1 Methods of Measuring Combustion Efficiency

Various methods have been used to attempt to measure combustion efficiency of flares in crosswind. These include:

- Aerial approaches, e.g. using drones
- Remote optical, e.g. using passive Fourier transform infrared (FTIR) and differential absorption light detection (DIAL) techniques
- Extractive probe sampling from full sized flare plumes
- Wind tunnel
    - Single pass
    - Closed loop

Obtaining representative samples of the complete combustion products is a potential issue for the drone and extractive sampling approaches. One study [5] has compared various optical methods against one another and also with the extractive sampling approach and found significant disagreement when measuring the same flare.

These problems are exacerbated under windy conditions. For example, it has been observed that packets of uncombusted flare gas can be emitted on the underside of the wind-deflected flame, separate from the main plume of hot products [1].

The mixing of dilution air from the atmosphere is also an issue for the extractive sampling and single pass wind tunnel approaches. The level of dilution can be calculated but this increases the uncertainty in the calculated combustion efficiency.

The point of extraction and measurement is important as the variation in combustion efficiency at various points in the flare plume varies widely. This is illustrated in Figure 1 and Figure 2 (reproduced from [1]) which are contour plots of the relative concentration levels of the combustion products, CO2, CO and unburned hydrocarbons, encountered in the flare plume:

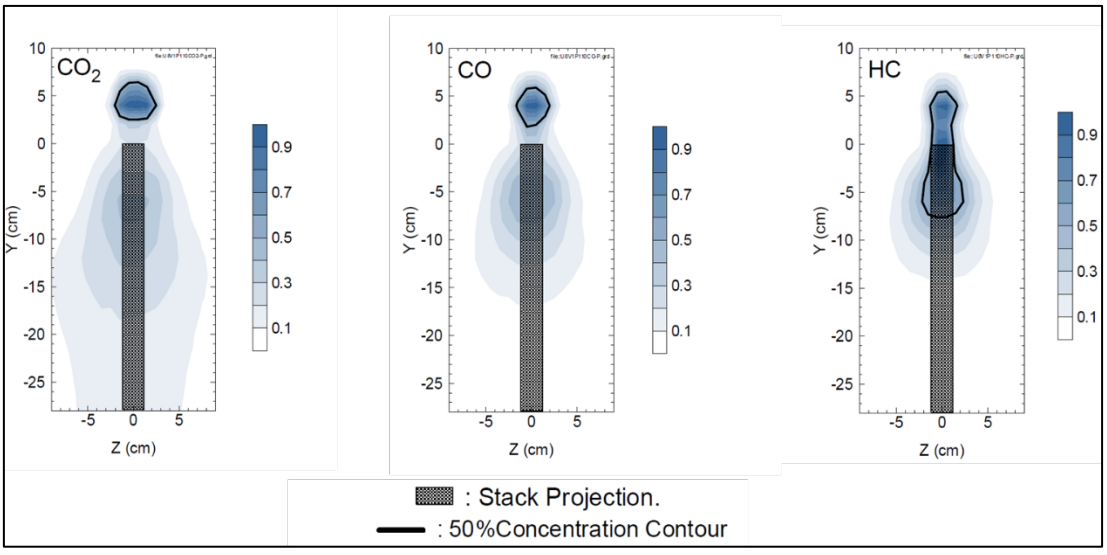

Figure 1 Variation in relative concentration of combustion products, stack projection

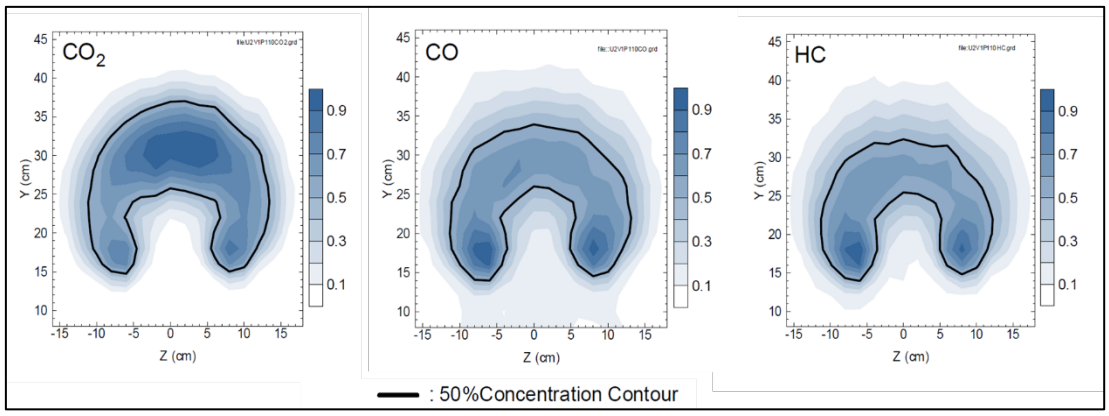

Figure 2 Variation in relative concentration of combustion products, plan view

Figure 1 plots the variation of the combustion products in a vertical plane viewed in the same direction as the wind. This illustrates the significant variation in the spatial distribution of the flare products. Of note, are the two peaks in concentration, one above the stack and one below its tip, on the leeward side of the flare. This is due to packets of uncombusted hydrocarbons escaping from the flare plume caused by a standing vortex on the downwind side of the flare generated by the crosswind.

Similar variation and multiple peaks in concentration are observed in the horizontal plane (plan view) in Figure 2.

The resultant spatial distribution of combustion efficiency is presented in Figure 3.

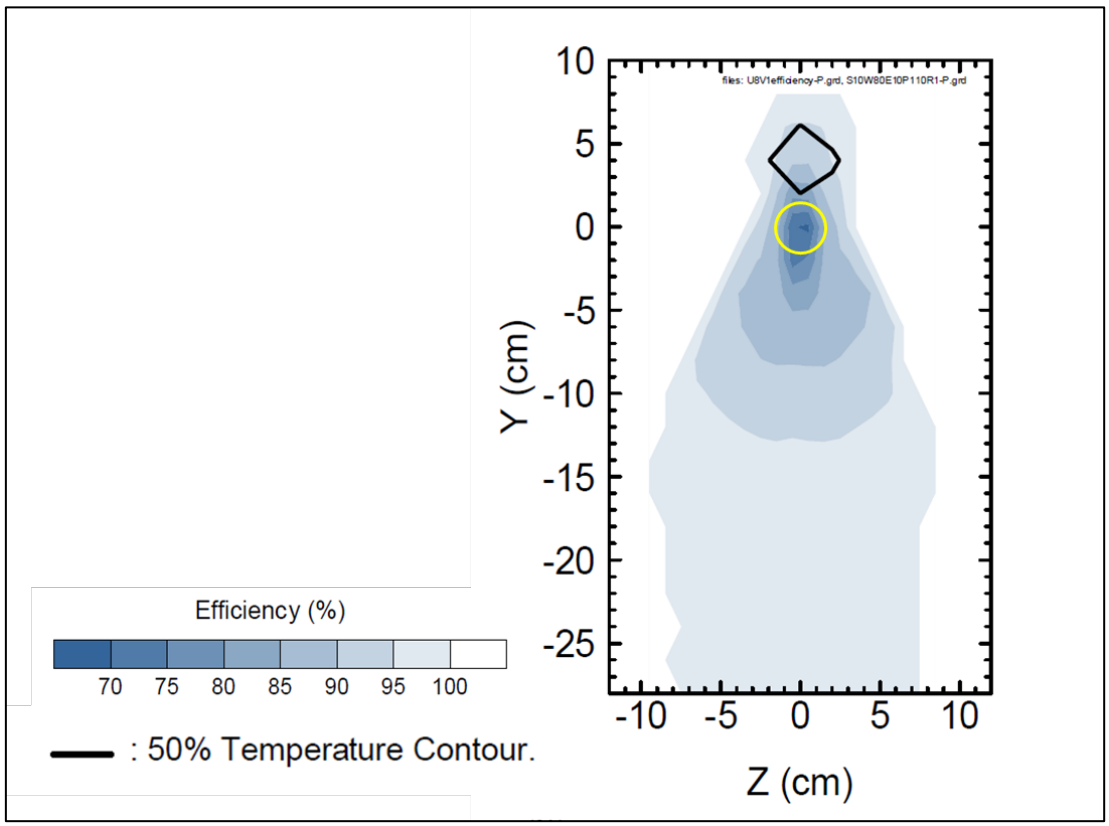

Figure 3 Variation in combustion efficiency, plan view

As can be observed there is a wide variation in the combustion efficiency over the plume. The yellow circle indicates the location of the flare stack.

The best method to capture all the combustion products and hence determine combustion efficiency over the whole plume is to enclose the flare in a wind tunnel. The wind tunnel methods provide the best method of capturing representative samples, though their challenge is scale, as the maximum size of flare analysable is limited by the physical dimensions of the wind tunnel.

2.2 UoA Combustion Efficiency Measurement Methodology

Currently, it appears that the most controlled method of measuring combustion efficiency from flares in a crosswind employs the use of a wind tunnel [6]. The UoA conducted research on combustion efficiency using a wind tunnel over several years, the results of which are described in a report published in 2004 [1].

The closed loop wind tunnel wide overcomes the variability of combustion efficiency (CE) around the flame as it samples the combustion products sufficiently downstream of the flare to ensure they are well mixed and representative of the whole flare combustion products. It is also less affected by air dilution than the other methods.

The enclosed nature of the tunnel, though reducing air dilution from the atmosphere, results in the concentration of the combustion products rising with time, rendering the calculation of the combustion efficiency more complicated. However, the dynamic nature of the measurements in fact provides advantages in that it reduces the uncertainty in the calculated CE and mitigates the impact of systematic uncertainties in the measurement instruments.

A high-level description of the UoA methodology used to calculate CE is provided below. The compete details of the calculations are provided in the UoA flare research final report [1] and associated paper [6].

Figure 4 is a simplified schematic of the closed loop tunnel with a flare burning.

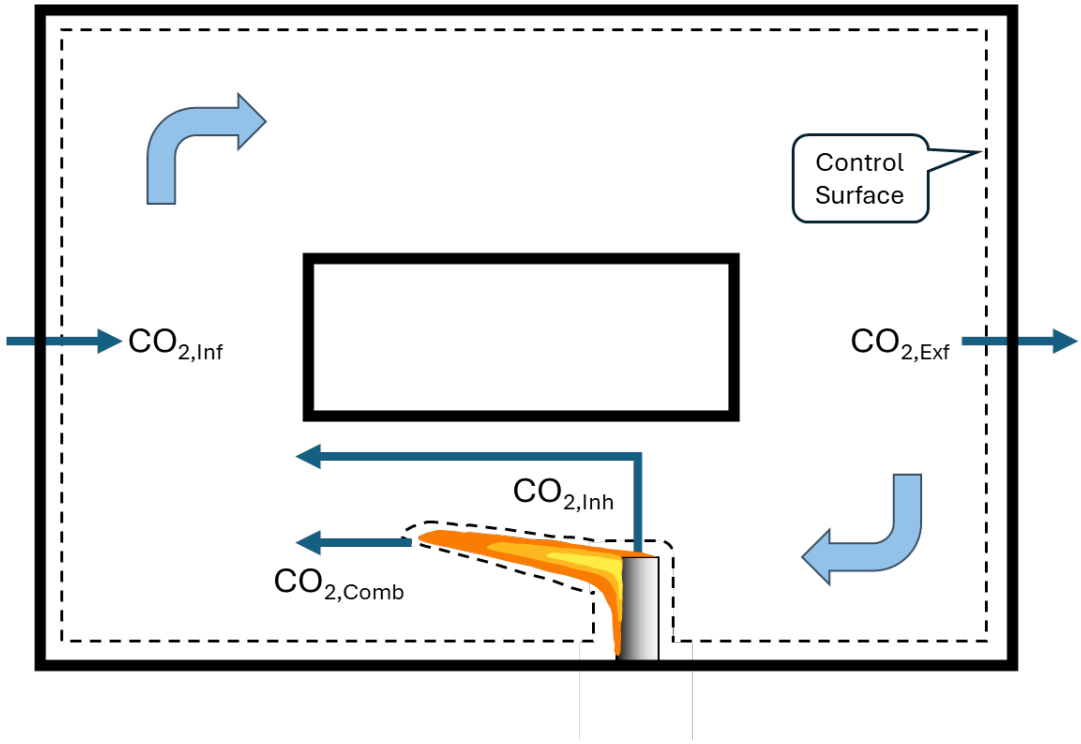

Figure 4 Schematic of a flare burning in a closed loop wind tunnel

The figure also depicts the main inflows and outflows of CO2 to/from the wind tunnel. A control surface is also indicated across which mass balances can be established. In the schematic, CO2 is used as an example, but the analysis is applicable to any of the component species present.

CO2 enters the wind tunnel due to combustion of the flare gas. CO2 may also be present inherently in the flare gas itself.

The use of a closed loop tunnel reduces the influx of dilution air, but it doesn't eliminate it and hence leakage of air into the tunnel occurs. Similarly, the wind tunnel gases leak out of the tunnel. Both need to be accounted for in the mass balance.

Also, the closed loop nature of the wind tunnel results in a dynamic situation as the recirculated air and combustion products cause the concentrations of the various reactants and products of combustion to change with time.

The quantity of CO2 in the tunnel can be described as:

Accumulation of CO2 in the tunnel =
CO2 produced by flare combustion
+ CO2 inherent in flare gas
+ CO2 in air infiltrated into tunnel
– CO2 lost due to leakage from tunnel
More formally, this is expressed by the following equation:

$$\frac{dm_{CO2}}{dt} = \dot{m_{CO2,Comb}} + \dot{m_{CO2,Inh}} + \dot{m_{CO2,Infil}} - \dot{m_{CO2,Exfil}} \qquad (1)$$

Where,

m_{CO2}	mass of CO2 in the tunnel (kg)
$\dot{m}_{CO2,Comb}$	mass flow of CO2 produced by combustion (kg/s)
$\dot{m}_{CO2,Inh}$	mass flow of CO2 inherent in the fuel gas (kg/s)
$\dot{m}_{CO2,Infl}$	mass flow of CO2 into the tunnel due to leakage (kg/s)
$\dot{m}_{CO2,Exfl}$	mass flow of CO2 out of the tunnel due to leakage (kg/s)

(Other factors affecting the mass balance were also taken into consideration by the UoA, including the addition of CO2 due to reburning of products (recycled round tunnel) and soot formation. However further analysis found that the impact of these quantities was negligible and could be discounted).

The inflow and outflow terms are difficult to determine. However, since the volume of the tunnel is constant a further constraint can be introduced and the volume flows of the gas entering and leaving the tunnel can be equated.

Consequently, the temperature inside the tunnel must be accounted for, as the gases in the tunnel are heated by the combustion process, causing their density to fall. The temperature increase during an experimental run was around 3°C.

Additionally, this volume balance introduces the internal volume of the tunnel in the equations. Though this known to be approximately 350 m^3, it is in fact difficult to determine to sufficient accuracy.

By formulating similar mass balances for carbon monoxide and the hydrocarbon content a set of three differential equations could be formulated, which when combined and rearranged, eliminated the problem terms, and resulted in the following equation for the combustion efficiency in terms of the rate of accumulation of CO2, CO and HC, all of which are accurately measurable:

$$\mu = \frac{\left(\frac{B}{A+C}\right) - \left(\frac{Y_{CO_2}}{m * Y_{C_mH_n}}\right)}{1 + \left(\frac{B}{A+C}\right)} \tag{2}$$

Where,

$$A = \frac{d}{dt}\left(\frac{Y_{HC}}{T}\right)\Big|_{t \to t'} \tag{3}$$

$$B = \frac{d}{dt}\left(\frac{Y_{CO_2}}{T}\right)\Big|_{t \to t'} \tag{4}$$

$$C = \frac{d}{dt}\left(\frac{Y_{CO}}{T}\right)\Big|_{t \to t'} \tag{5}$$

Where,

μ	combustion efficiency
A	rate of change of hydrocarbon mole fraction divided by temperature ($K^{-1}s^{-1}$)
B	rate of change of CO_2 mole fraction divided by temperature ($K^{-1}s^{-1}$)

C	rate of change of CO mole fraction divided by temperature ($K^{-1}s^{-1}$)
Y_{HC}	mole fraction of hydrocarbons in the tunnel
Y_{CO}	mole fraction of carbon monoxide in the tunnel
Y_{CO_2}	mole fraction of carbon dioxide in the tunnel
$Y_{C_mH_n}$	mole fraction of hydrocarbons in the tunnel
m	carbon number
n	hydrogen number
T	tunnel temperature (K)
t	time (s)
t'	end time (s)

A plot, based on data presented in [1], is reproduced below which illustrates the change in concentration of CO2, CO and HC with time for a typical experimental run:

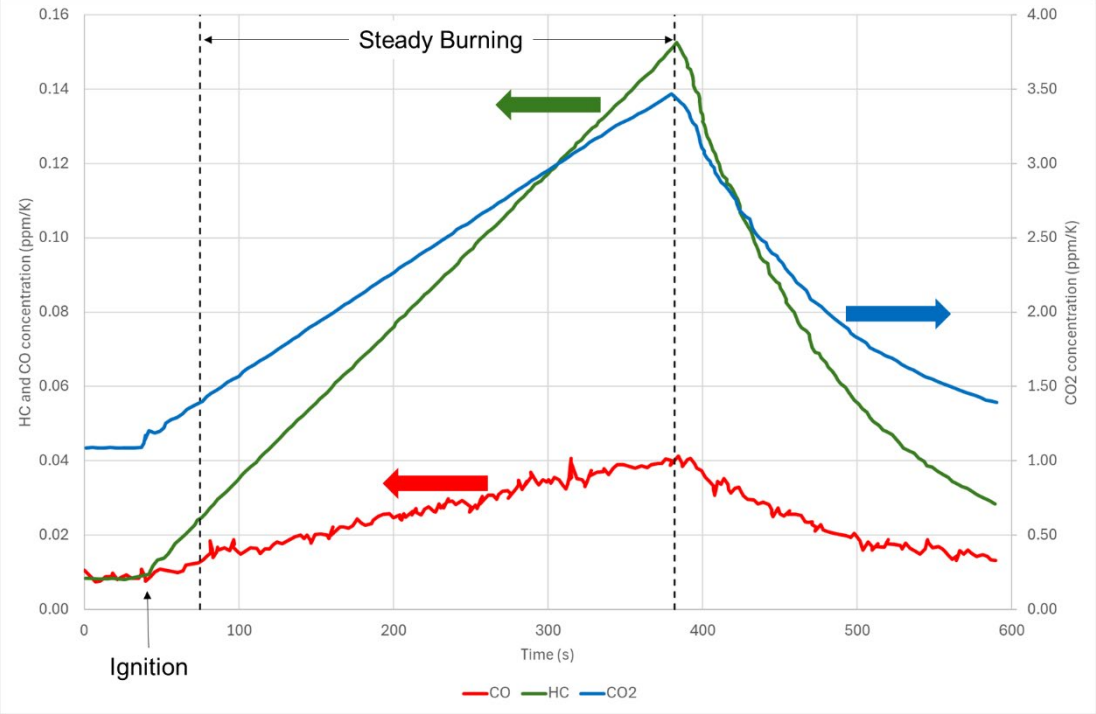

Figure 5 Temporal plots of concentrations of CO2, HC and CO during an experiment in the closed-loop wind tunnel

The advantage of this approach is that it is the slopes of the concentration changes of CO2, CO, and HC that are the input variables in the efficiency calculations. The slopes of the traces can be determined much more accurately than single point concentration readings which are more susceptible to drift and noise. This is why the closed loop tunnel is considered to be a more accurate approach to determining CE than using single pass open tunnels.

Because each of the slope terms appears in the numerator and denominator of equation (2), the effect of any errors tends to cancel which further mitigates the influence of the errors in the measurements.

The UoA conducted a detailed sensitivity and uncertainty analysis of this closed-loop wind tunnel methodology for measuring efficiencies of flares which is described in [6]. This analysis included consideration of the effects of errors in:

- CO2 in flare fuel gas composition
- CO2 slope
- CO slope
- HC slope

The combustion efficiency and associated uncertainties for two test cases from [6] are reproduced in Table 1:

Table 1 –Uncertainties in the Calculated Efficiency for Test A and B

Test	Combustion Efficiency	Absolute Uncertainty (99%)	Absolute Uncertainty (95%)
Test A	97.18%	±0.06%	±0.05%
Test B	91.79%	±0.14%	±0.11%

The UoA reported their uncertainties at the 99% confidence level, these have also been expressed at the 95% confidence level more commonly used in the oil and gas industry.

To cover a wider range of combustion efficiencies, the author developed a methodology to estimate the uncertainty in the UoA measurements based on equation (2) and the data in the two test cases above. This allowed the absolute uncertainty to be estimated for a more extended range of CE values plotted in Figure 6:

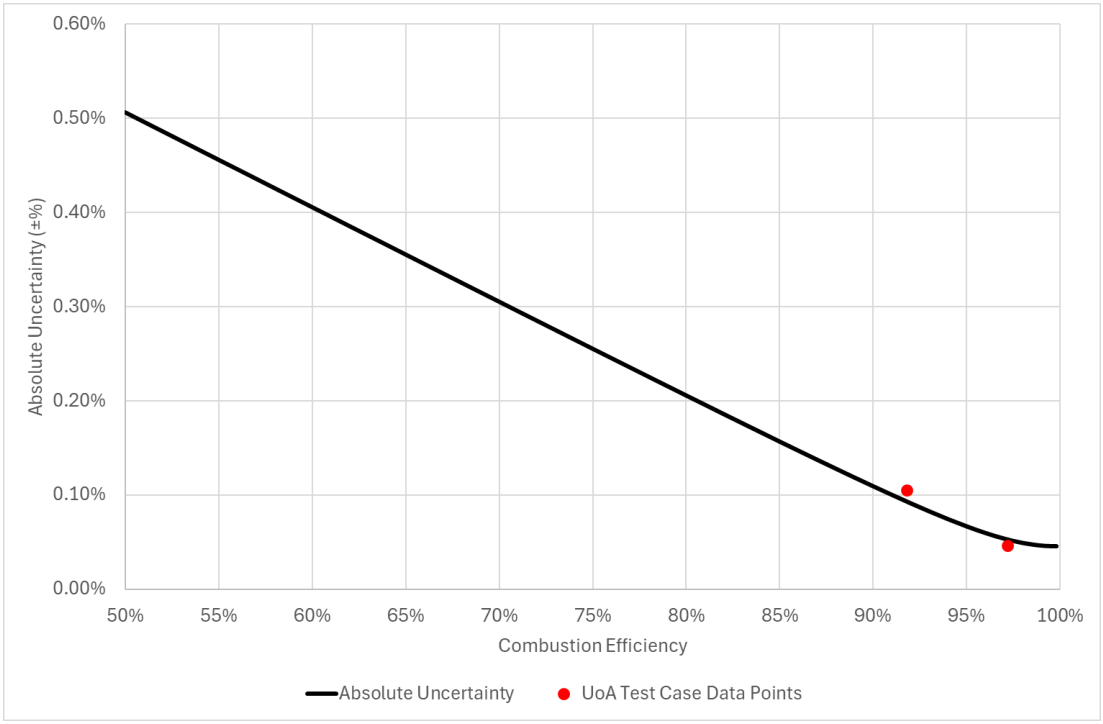

Figure 6 Approximate Absolute Uncertainty in CE Measurement

The uncertainty in the CE measurement rises as the CE itself reduces. However, the plot illustrates that the uncertainty in the measurements of combustion efficiency were relatively low and do not contribute significantly to the scatter of the data points about the UoA combustion efficiency equation discussed in the next section.

3 UoA COMBUSTION EFFICIENCY EQUATION UNCERTAINTY

One of the products of the research was the development of a semi-empirical equation that calculates combustion efficiency as a function of fuel type, wind speed, flare jet exit velocity, flare stack outside diameter and the specific energy content of the fuel mixture, expressed in terms of the mass based lower (or net) heating value (LHV).

The methodology and development of the relationship are described in [1], [7] and [8]. The resultant relationship is of the form:

$$\mu = 1 - \alpha \left(\frac{LHV_{CH4}}{LHV_f} \right)^3 e^{\left(\frac{\beta U_w}{(gdU_f)^{1/3}} \right)} \quad (6)$$

Where,

μ	combustion efficiency
LHV_{CH4}	mass based lower heating value methane (MJ/kg)
LHV_f	mass based lower heating value flare stream (MJ/kg)
U_w	wind speed (m/s)
U_f	flare jet exit speed (m/s)
g	acceleration due to gravity (m/s^2)
d	flare outer diameter (m)
α	coefficient of linear fit
β	coefficient of linear fit

The two constants, α and β, were determined based on the data from the wind tunnel, which measured the CE over a series of experiments that varied:

- Wind speed, U_w
- LHV of the flare gas, LHV_f
- Velocity of the flare gas, U_f
- Diameter of the flare, d

Using dimensional analysis, the researchers were able to express the CE in terms of two dimensionless groups: a modified Richardson Number and an energy density group.

The modified Richardson number is given by:

$$\Omega = \frac{U_w}{(gdU_f)^{1/3}} \quad (7)$$

This is an expression of the ratio of flow shear (due to the cross wind) and buoyancy (of the flare plume).

The energy density number is simply expressed in terms of the flare gas Lower Heating Value (LHV) relative to that of methane:

$$N_E = \left(\frac{LHV_f}{LHV_{CH4}} \right) \quad (8)$$

Rearranging equation (6):

$$(1-\mu)\left(\frac{LHV_f}{LHV_{CH4}}\right)^3 = \alpha e^{\left(\frac{\beta U_w}{(gdU_f)^{1/3}}\right)} \quad (9)$$

This can be expressed in terms of the Richardson number Ω and another dimensionless quantity Ψ:

$$\Psi = \alpha e^{(\beta\Omega)} \quad (10)$$

Where,

$$\Psi = (1-\mu)\left(\frac{LHV_f}{LHV_{CH4}}\right)^3 = (1-\mu)(N_E)^3 \quad (11)$$

The data is plotted in terms of these two dimensionless quantities for natural gas flares:

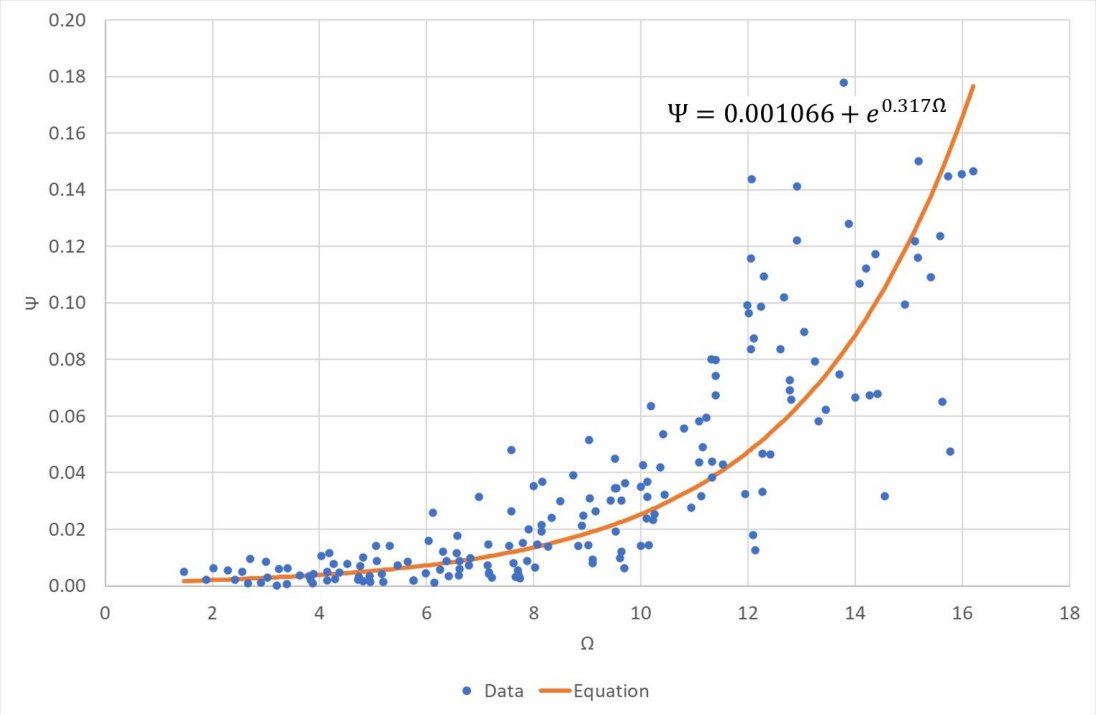

Figure 7 UoA data plotted in terms of Ψ and Ω

By taking logs a linear relationship can be established:

$$\ln(\Psi) = \ln\alpha + \beta\Omega \quad (12)$$

When plotted:

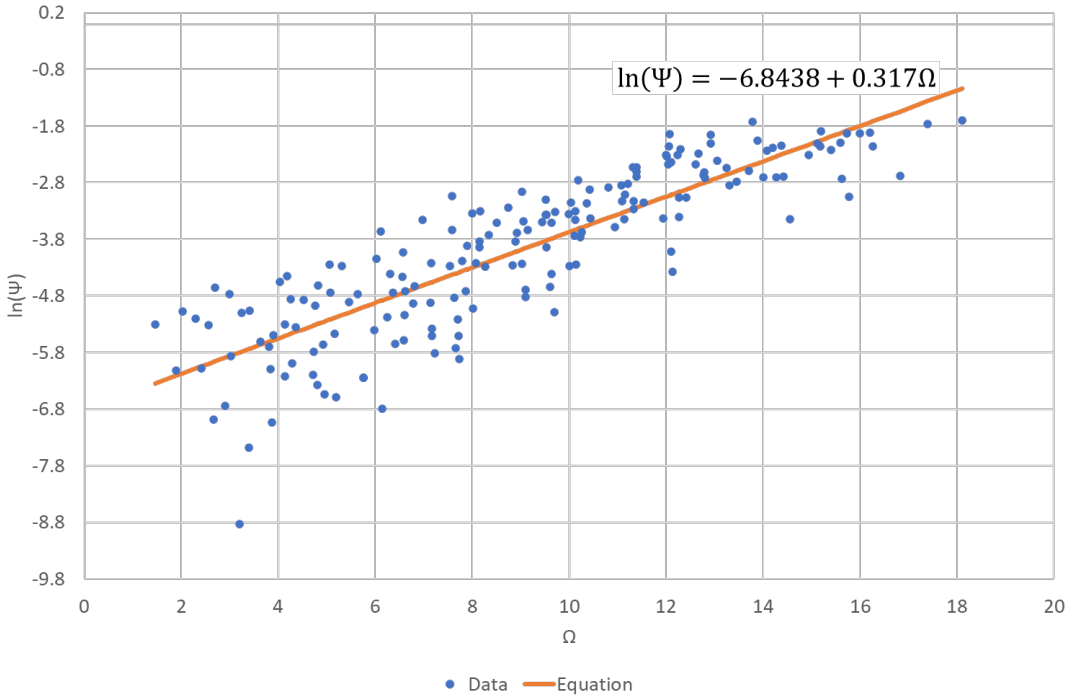

Figure 8 UoA data plotted in terms of $\ln \Psi$ and Ω

A least squares regression produced the equation indicated by the orange line in Figure 8.

Figure 7 includes a transformed version of the equation indicated by an orange line also, which is reproduced below:

$$\mu = 1 - 0.001066\left(\frac{LHV_{CH4}}{LHV_f}\right)^3 e^{\left(\frac{0.317U_w}{(gdU_f)^{1/3}}\right)} \qquad (13)$$

These constants:

$\alpha = 0.001066$

$\beta = 0.317$

are applicable for natural gas flares.

The UoA wind tunnel tests were performed on flares up to 2" diameter. The results were combined with those from combustion efficiency measurements taken at the National Research Council (NRC) in Ottawa, using a single pass wind tunnel on flares up to 4" diameter, also described in [1].

As stated above, the two constants in Equation (13) were derived from a least squares regression of such measurements. The variance, covariance and uncertainty in these constants was determined and the results presented in Table 1:

Table 1 – Variance, Covariance and Uncertainty UoA Equation Constants

Parameter	UoA Value	Data Extract Value	Variance / Covariance	Absolute Uncertainty
Constant ln(A)	-6.8438	-6.8003	0.018556	0.2670
Constant B	0.317	0.313	0.000193	0.0272
Covariance ln(A) and B			-0.00174	

The covariance term is important as it has a significant effect on the uncertainty of calculated values of CE generated using the equation.

The source data was not directly available, so the data points were obtained using a web-based utility to extract data from images of charts [9]. The curve fit was reproduced using data extracted from Figure 8.6 in the UoA report [1]. The values of the constants from this exercise are presented above and closely match the UoA values. The regenerated curve-fit additionally allowed the variance and covariance statistics to be obtained and which can be assumed to be representative of the original equation.

The variance/covariance in the constants can be used to generate an uncertainty associated with the equation itself. This is described in the GUM [10], most explicitly in example H.3.

4 UNCERTAINTY IN FIELD MEASUREMENT COMBUSTION EFFICIENCY

4.1 UoA Equation Input Variables

In operation the measurement or calculation of the flare LHV, exit velocity, flare diameter and wind speed will introduce additional uncertainty into the calculated CE.

These four input parameters are all individually measured or simulated and hence are independent of one another.

The uncertainty in exit velocity, flare diameter and wind speed may be obtained based on manufacturer information and conventional methods. The flare exit velocity and windspeed uncertainties can be updated dynamically, whereas flare dimensions remain static.

The uncertainty in LHV is more difficult to measure directly and is discussed in the next section.

4.2 Uncertainty in Lower Heating Value

To determine the LHV, the flare gas may be sampled, and its composition determined, via an online gas chromatograph if one is installed or, more commonly, sampled intermittently and analysed in a laboratory.

Since gas can be routed to the flare from many points in the process, the compositional variation could potentially be wide.

The problem with intermittent samples is that they may not adequately capture the variation in the flare gas composition. However, retrofitting online chromatographs on existing flares may be costly or difficult to achieve.

Additionally, nitrogen or fuel gas purges of the flare stack can be downstream of the sample point.

An alternative is to simulate the flare stream composition based on live operational process data and hence determine its LHV. The entire topsides process is simulated and updated using live process operating conditions, measured feed rates, etc.

At the heart of Combustor is the Accord CHARM process simulation software. CHARM predicts the composition and lower heating value of the flared gases immediately prior to combustion and accounts for any nitrogen or fuel gas purge streams which might enter the flare gas system downstream of final stage production equipment such as flare knock out drums.

The use of simulations to predict flare compositions and associated properties is described in our previous paper [4]. The paper also describes the calculation of the associated uncertainties using CHARM and employing the Monte Carlo Method (MCM), which is described in a Supplement to the GUM [3]. The LHV on a mass basis, as employed in the UoA equation, exhibits a relatively low uncertainty. This is because the mass based LHV of the alkanes are all relatively similar in magnitude. The LHV asymptotically falls towards to a constant value with increasing carbon number.

To illustrate the accuracy of simulated LHVs, Figure 9 compares the CHARM LHV with the LHV calculated from samples obtained from a platform operating in the North Sea.

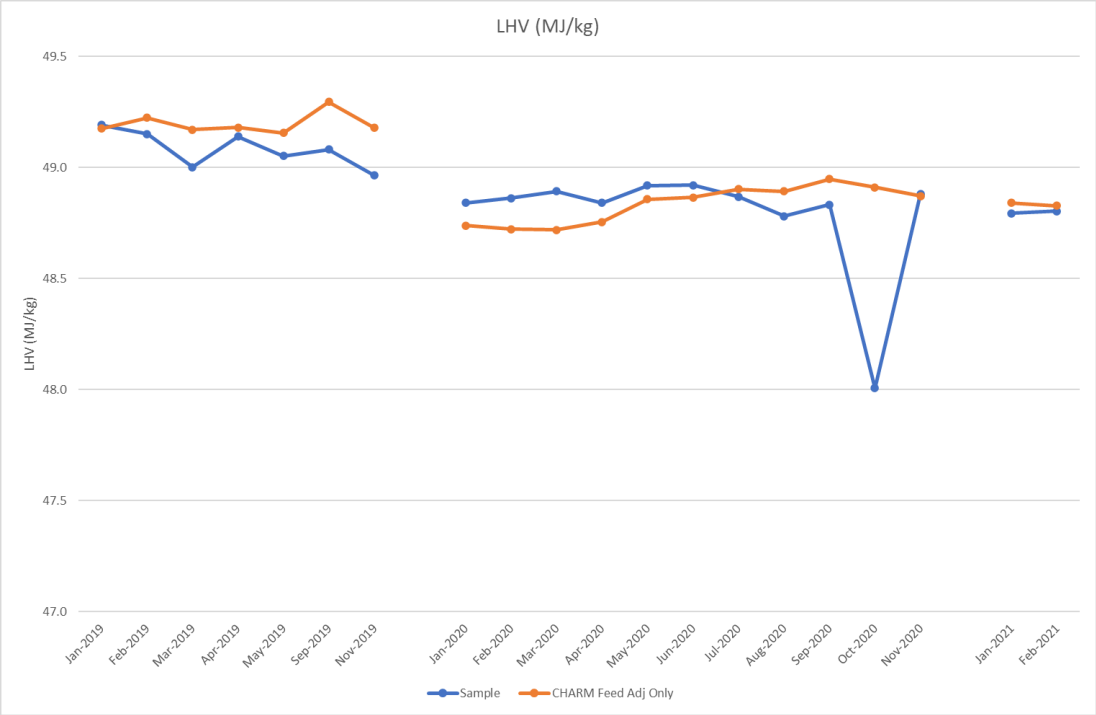

Figure 9 CHARM Simulated LHV Compared with LHV from Sampled Compositions

The simulated LHVs are typically within 0.2 MJ/kg of the sampled values, except for an apparent outlier in Oct-2020, confirming the viability of using process models to calculate flare LHV. The uncertainty in the CHARM LHV was calculated to be ±0.6% relative or ±0.3 MJ/kg absolute.

4.3 Uncertainty Calculation Methodology

The contribution of all the input parameters, including that of the UoA equation itself, to the total CE uncertainty comprises two elements (as described in the GUM [10]):

- The uncertainty in the measured or estimated parameter (U_i)
- The sensitivity of the CE to the parameter (C_i)

The sensitivity coefficients (partial differentials) were determined analytically (and cross-checked numerically).

The covariance terms associated with the UoA constants also need to be included in the uncertainty calculation of the CE.

4.4 CE Uncertainty Sensitivity Analysis

To understand the sensitivity of the combustion efficiency and its associated uncertainty to the magnitude and uncertainty of the input variables a parametric study has been performed.

The uncertainty on the predicted CE has been calculated over a range of values for each of the input quantities.

A base case has been established which has the following parameter values:

Table 2 – Base Case Input Variable Values and Uncertainties

Parameter	Units	Value	Relative Uncertainty (± %)
LHV	MJ/kg	49.03	0.54%
Wind Speed	m/s	10.0	2.0%
Flare Exit Velocity	m/s	1.0	7.5%
Flare Outside Diameter	m	0.40	0.2%

As discussed in [4], 10 m/s is approximately the average wind speed experienced in the North Sea.

For this case the CE is calculated to be 99.16%, with an uncertainty of +0.12%, -0.13% in absolute terms. The uncertainty is asymmetrically distributed because of the logarithmic nature of the UoA equation least squares regression as illustrated in Figure 10.

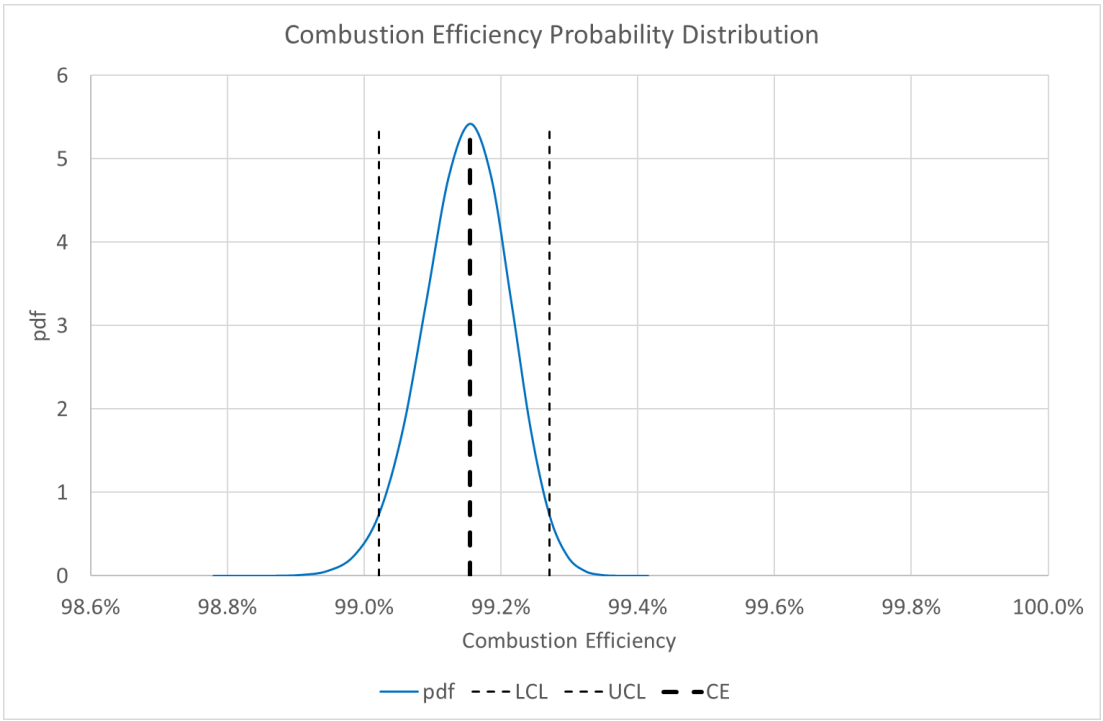

Figure 10 CE Uncertainty Probablility Distribution for Base Case, Wind Speed 10 m/s

If the wind speed is significantly increased, the CE falls and the uncertainty bands widen as illustrated in Figure 11:

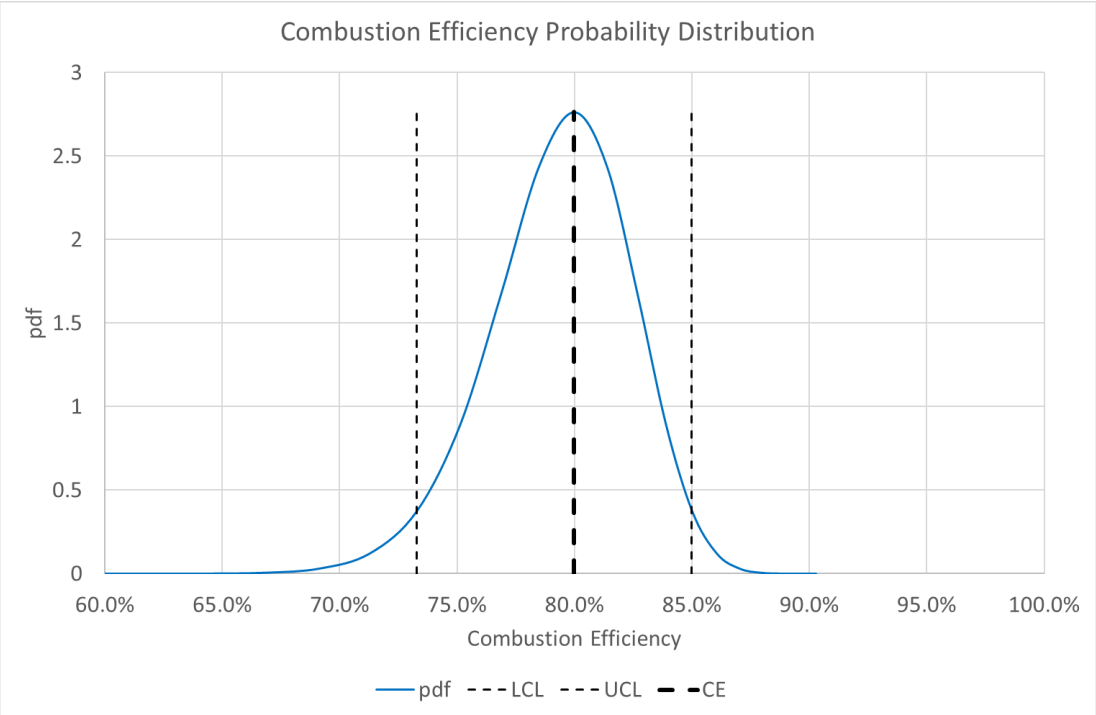

Figure 11 CE Uncertainty Probablility Distribution for Base Case, Wind Speed increased to 25.8 m/s

The CE decreases to 80.0% +5.0%, -6.7%; the asymmetry is now more pronounced.

A general feature of the calculated CE uncertainty is that as the CE falls the uncertainty in the result increases.

The importance of accounting for the covariance term in the UoA coefficients is illustrated in Figure 12, which plots the uncertainty distribution with the covariance term (incorrectly) ignored.

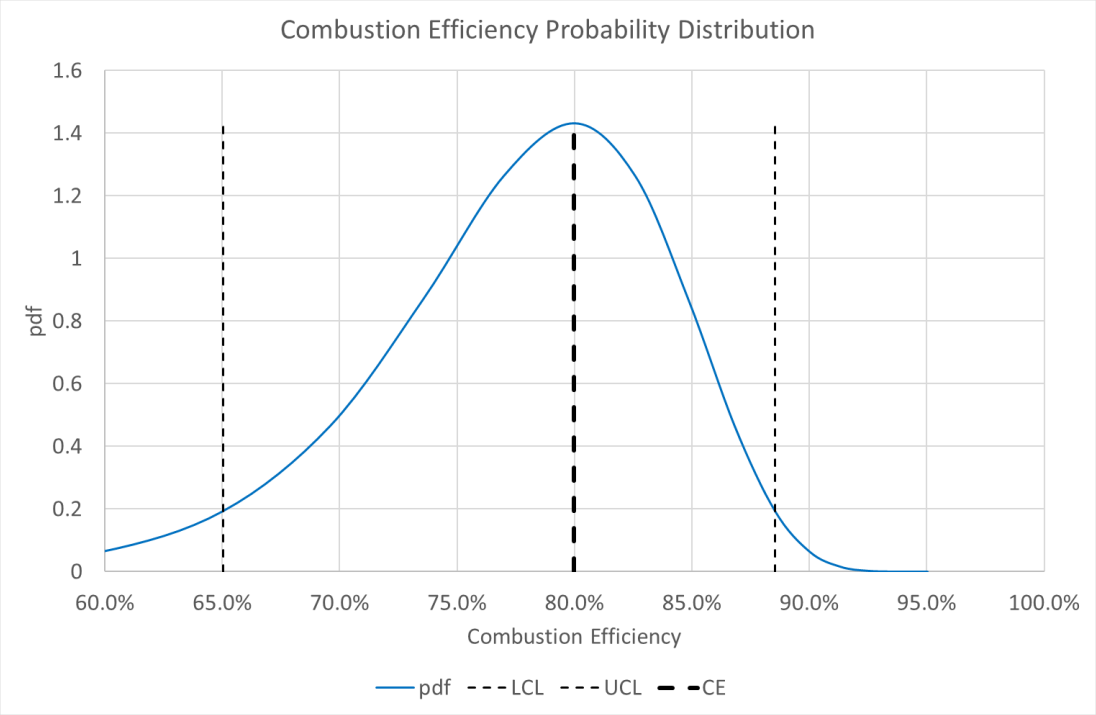

Figure 12 CE Uncertainty Probablility Distribution for Base Case, Wind Speed increased to 25.8 m/s, UoA Coefficient Covariance Excluded

The uncertainty is now incorrectly over-estimated to be +8.6%, -14.9%.

The covariance term reduces the overall uncertainty because it has a negative value.

A sensitivity analysis was conducted which varied each of the input variables over a range of possible values:

Table 3 – Parametric Study Input Variable Range of Values

Parameter	Units	Minimum	Maximum
LHV	MJ/kg	10.0	50.0
Wind Speed	m/s	0.0	30.0
Flare Exit Velocity	m/s	0.05	2.5
Flare Outside Diameter	m	0.10	2.0

The results are presented in the form of charts in the next four sub-sections. The top chart in each section is a bar chart that plots the absolute uncertainty in CE over the range of values for the input parameter being varied. The remaining parameters are held constant at their base case value.

The contribution to the CE uncertainty of each of the variables is also shown in the stacked bar.

The contribution of each parameter is estimated by recalculating the CE with the uncertainty in that parameter set to zero and observing the drop in CE uncertainty, the magnitude of the drop is proportional to the parameter's influence on the uncertainty. This is carried out for each of the parameters. The individual contributions, so calculated, do not sum to the total CE

uncertainty and are therefore scaled down to do so. (It is the variances and the squares of the sensitivity coefficients that are additive, but these are not so intuitive to consider).

The contribution of the UoA equation is also included in the analysis.

The lower line chart plots the corresponding CE values and along with error bars representing the uncertainty at each point.

4.4.1 LHV

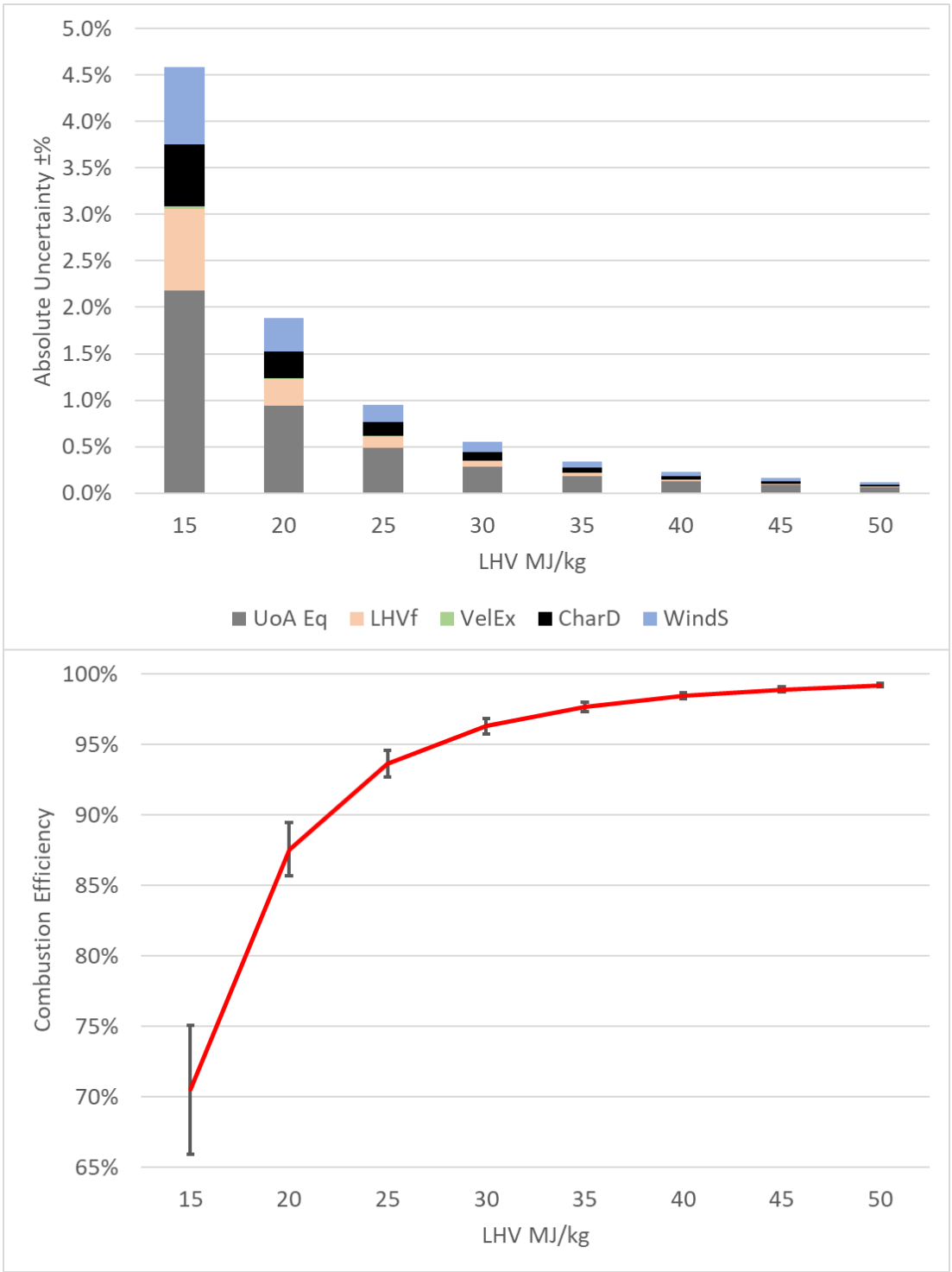

Figure 13 CE and Associated Uncertainties, LHV Sensitivity

4.4.2 Wind Speed

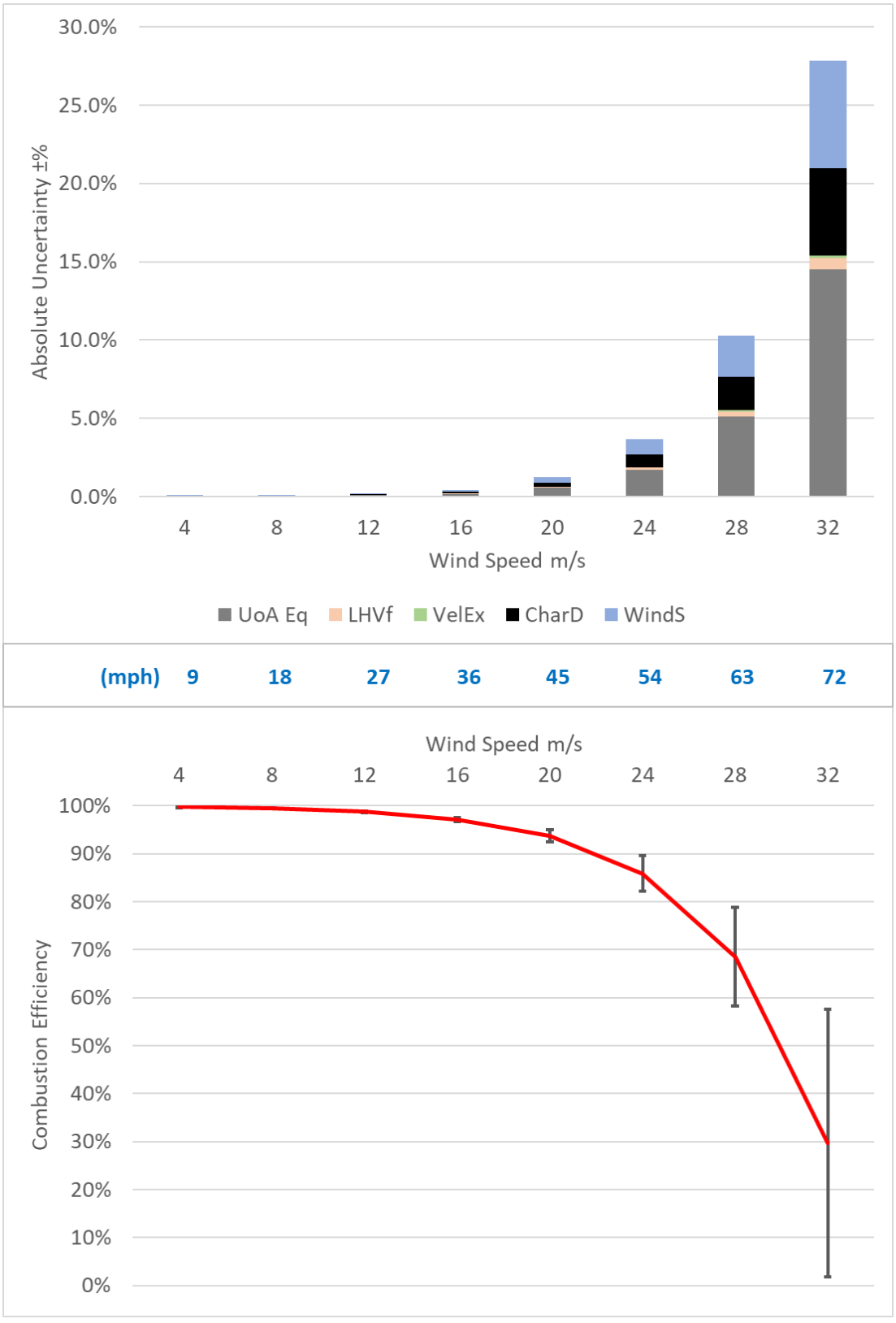

Figure 14 CE and Associated Uncertainties, Wind Speed Sensitivity

4.4.3 Flare Exit Velocity

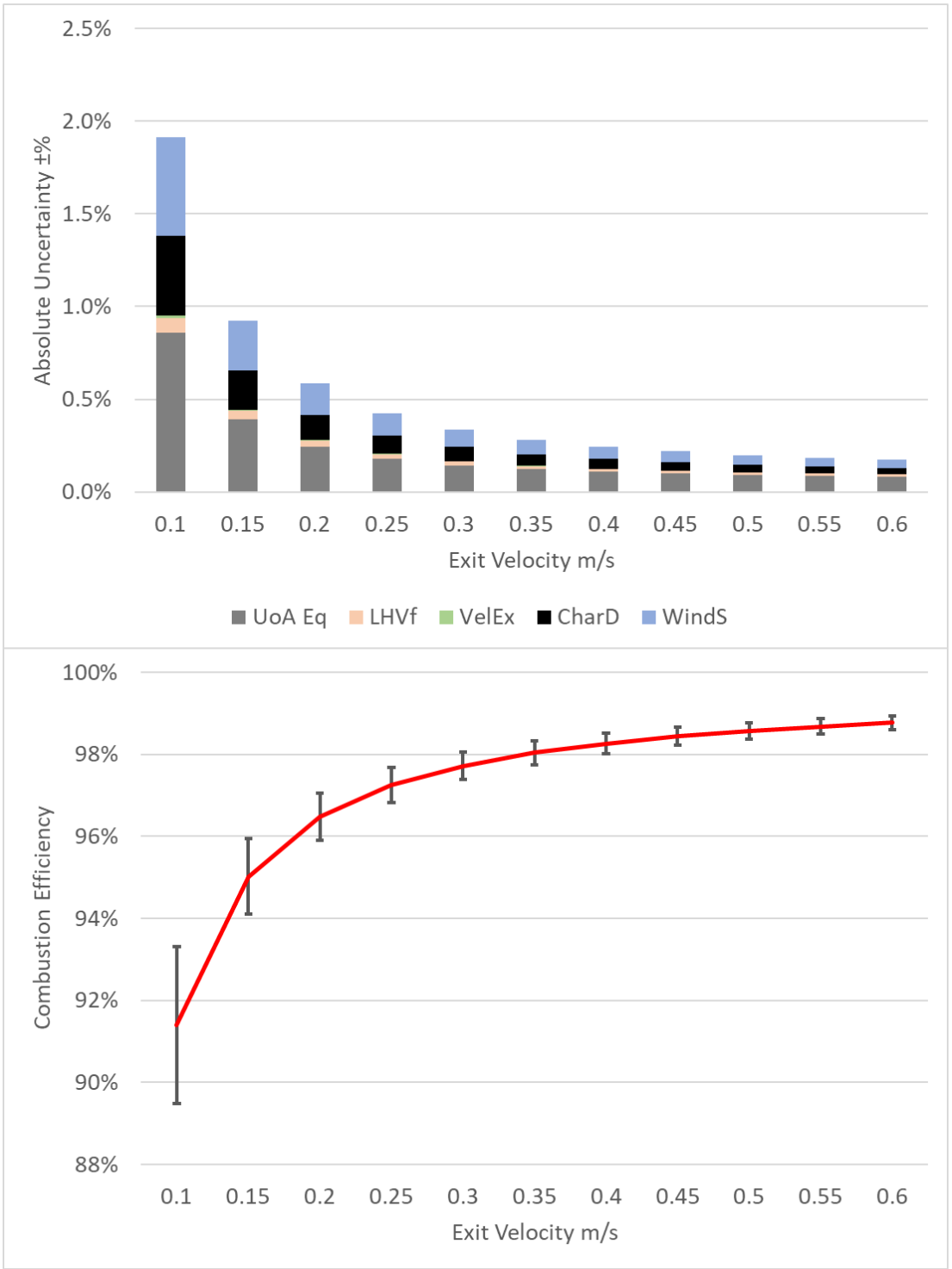

Figure 15 CE and Associated Uncertainties, Flare Exit Velocity Sensitivity

4.4.4 Flare Diameter

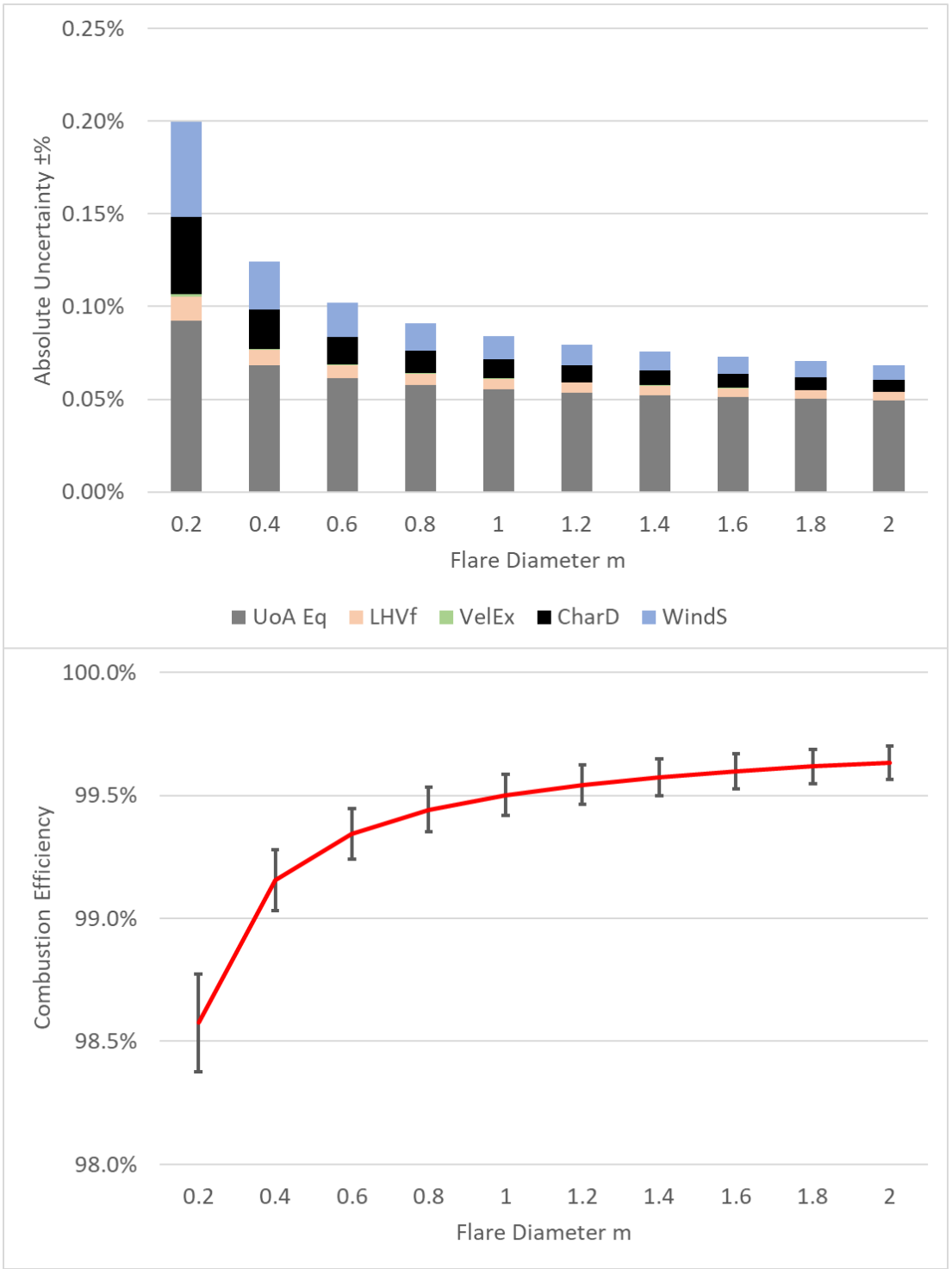

Figure 16 CE and Associated Uncertainties, Flare Diameter Sensitivity

4.4.5 Discussion

The key features of the above analysis are listed below.

The uncertainty in CE increases as CE itself decreases.

CE decreases with:

- increasing windspeed
- decreasing LHV, flare exit velocity and flare diameter.

This is explained to some extent by the form of Figure 7, which plots a combination of the flare inefficiency (100% minus CE) and the LHV of the flare gas, represented by Ψ against the modified Richardson Number Ω. At low values of both Ψ and Ω the scatter of the experimental data points is much less than at high values of these variables.

High values of Ψ occur at low CE and LHV values.

Ω is proportional to windspeed but inversely proportional to flare exit velocity and flare diameter. The less dramatic variation observed with flare exit velocity and flare diameter is because they are raised to the 1/3 power in Ω.

The contribution of the UoA equation itself is significant in all cases and hence is an important contributor that needs to be accounted for in the calculation of the CE uncertainty.

Also, the contribution of the parameters held constant in each set of cases changes. Their uncertainties do not change but the varied parameter has an impact on their sensitivity coefficients.

It is important and useful to understand the drivers of CE uncertainty, but perhaps the more important question is the impact they have on CO2e emissions, which is discussed in the next section.

5 UNCERTAINTY IN CO2e EMISSIONS

5.1 CO2e Calculation

The total emissions from the flare are the aggregate of the unburnt methane and the quantity of CO_2 that is emitted due to the combustion of hydrocarbons by the flare. This requires a relationship between methane and CO_2 in terms of global warming impact. This is provided by the Global Warming Potential (GWP) value. It is a measure of how much energy the emission of 1 ton of a gas will absorb over a given period of time, relative to the emission of 1 ton of carbon dioxide (CO_2).

The associated carbon dioxide equivalent or CO_2e means the number of metric tons of CO_2 emissions with the same global warming potential as one metric ton of another greenhouse gas.

The GWP of methane is multiple times that of CO_2. The GWP depends on the length of period it is specified over as methane has a half-life in the atmosphere of 11.8 years, whereas CO_2's half-life is considerably longer. The GWP of methane over 20 years is 81.2, meaning that a methane emission is projected to have 81.2 times the impact on temperature of a carbon dioxide emission of the same mass over the following 20 years. The GWP falls to 27.9 if taken over a 100-year period. Data from IPCC 6 report [11].

Also required is the composition of the unburnt gas as not all of it is necessarily methane. The fuel stripping mechanism suggests that the unburnt gas has the same composition as the flare gas and the UoA research team found this to be the case at higher wind speeds.

The total emissions in terms of CO_2e are given by:

$$M_{CO2e} = \mu_{DRE} E_{CO2e} Q_f \rho_f + (1 - \mu_{DRE}) GWP_{CH4} w_{CH4} Q_f \rho_f \quad (14)$$

Where,

μ_{DRE}	destruction removal efficiency of methane
M_{CO2e}	total mass flow of CO_2 equivalent emitted by the flare (kg/s)
Q_f	total volumetric flow of unburnt flare jet (m^3/s)
E_{CO2e}	mass of CO2 produced per mass of unburnt flare gas (kg/kg)
GWP_{CH4}	GWP of methane (kg/kg)

The first term is the mass of CO2 produced due to combustion of the flare gas and the second term represents the mass of unburnt methane emitted converted to an equivalent amount of CO2 in terms of Global Warming Potential.

The destruction removal efficiency figure is less than or equal to the combustion efficiency. However, the OGMP technical guidance document [2] states that the UoA CE equation may be used to estimate DRE in flares. Hence, the CE from Equation (13) can be substituted in (14) and if the flare exit velocity term is expressed in terms of the volumetric flow rate divided by the flare tip cross sectional area, the total CO_2e emissions are given by:

$$M_{CO2e} = Q_f \rho_f \left[\left(1 - 0.001066 \left(\frac{LHV_{CH4}}{LHV_f} \right)^3 e^{\left(\frac{0.317 U_w}{\left(\frac{g d Q_f}{A_f} \right)^{1/3}} \right)} \right) \times (E_{CO2e} - GWP_{CH4} w_{CH4}) + GWP_{CH4} w_{CH4} \right] \quad (15)$$

Where,

A_f	Cross sectional area of the flare tip (m^2)

5.2 CO2e Uncertainty

The uncertainty in this calculated CO_2e emissions flow rate can be determined using the techniques described in Section 4.3, i.e. in accordance with the GUM.

The base case from Section 4.4 has been extended to include the additional parameters in equation (15) and all variables are listed below:

Table 4 – CO2e Base Case Input Variable Values and Uncertainties

Parameter	Units	Value	Relative Uncertainty (± %)	Note
LHV	MJ/kg	49.03	0.54%	Covariant
Wind Speed	m/s	10.0	2%	
Flare Volumetric Flow	m^3/s	0.126	7.5%	
Flare Density	kg/m^3	0.752	0.56%	
ECO2	kg/kg	2.76	0.70%	Covariant
Flare C1 Content	wt%	84.5%	6.48%	Covariant
Flare Diameter	m	0.40	0.2%	
Flare Tip CSA	m^2	0.13	0.4%	
CH4 GWP-20	kg/kg	81.2	38%	
CH4 GWP-100	kg/kg	27.9	48%	

Though not listed above, the uncertainties and covariance in the UoA equation coefficients were included in the calculations.

The uncertainties for the LHV, ECO2 and C1 flare gas content were obtained from the CHARM simulation and therefore have covariance terms. The variance covariance matrix for these terms is presented in Table 5:

Table 5 – CHARM Variables Variance Covariance Matrix

	LHVf	WtfracCH4	ECO2
LHVf	0.017449	0.003587	-0.001266
WtfracCH4	0.003587	0.000749	-0.000263
ECO2	-0.001266	-0.000263	0.000093

The flare gas density can also be determined from the simulation but in this case, it has been assumed that it is obtained independently. Similarly, the flare tip cross sectional area (CSA) and flare diameter could be considered covariant but the characteristic diameter for the UoA equation is the outside diameter and not identical to that used to obtain the flare tip CSA.

The GWP values were obtained from Table 7.SM.6 and the uncertainties from 7.SM.8 of the Supplementary Material to Chapter 7: “The Earth’s Energy Budget, Climate Feedbacks, and Climate Sensitivity” of the IPCC Sixth Assessment Report, Working Group 1: The Physical Science Basis [11]. It should be noted that the uncertainties quoted in Table 4 are at the 95% confidence level (i.e. 1.96 standard deviations) whereas IPCC report’s figures are at the 90% confidence level (1.645 standard deviations).

For the base case, the CO2e emissions are calculated to be 0.279 kg/s (24.1 te/d), with an uncertainty of ±0.012 kg/s (±1.8 te/d) absolute and ±7.6% relative.

5.3 CO2e Uncertainty Sensitivity Analysis

For the base case, the principal contributor to the uncertainty is the flare meter itself. Therefore, a sensitivity analysis was conducted in which the uncertainty in volumetric flow was reduced, to determine the benefit gained from improved flow meter uncertainty. The results are plotted in Figure 17:

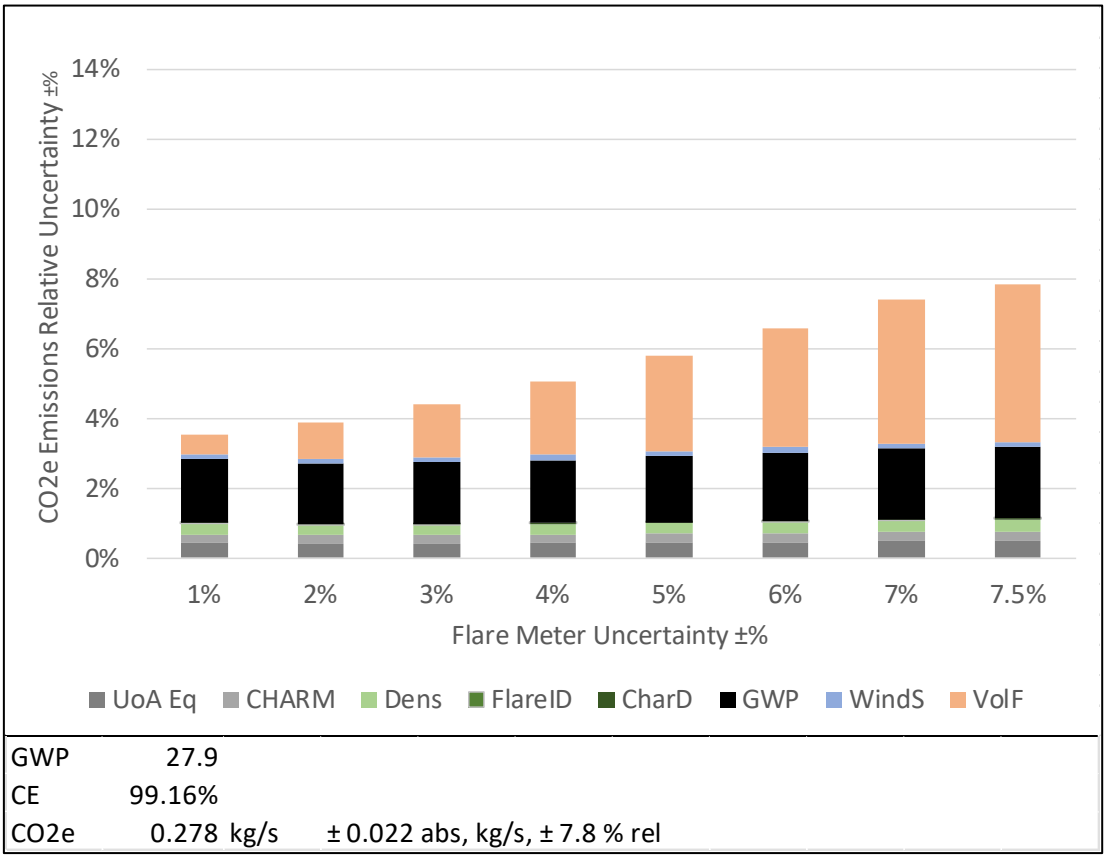

GWP	27.9		
CE	99.16%		
CO2e	0.278	kg/s	± 0.022 abs, kg/s, ± 7.8 % rel

Figure 17 CO2e Uncertainties, Flare Meter Uncertainty Sensitivity, Base Case GWP-100

Reducing the flare meter uncertainty does reduce the CO2e emissions uncertainty, but the effect levels off as the uncertainties in other parameters become more dominant, most notably the GWP. If the 20-year GWP value is adopted the analogous plot becomes:

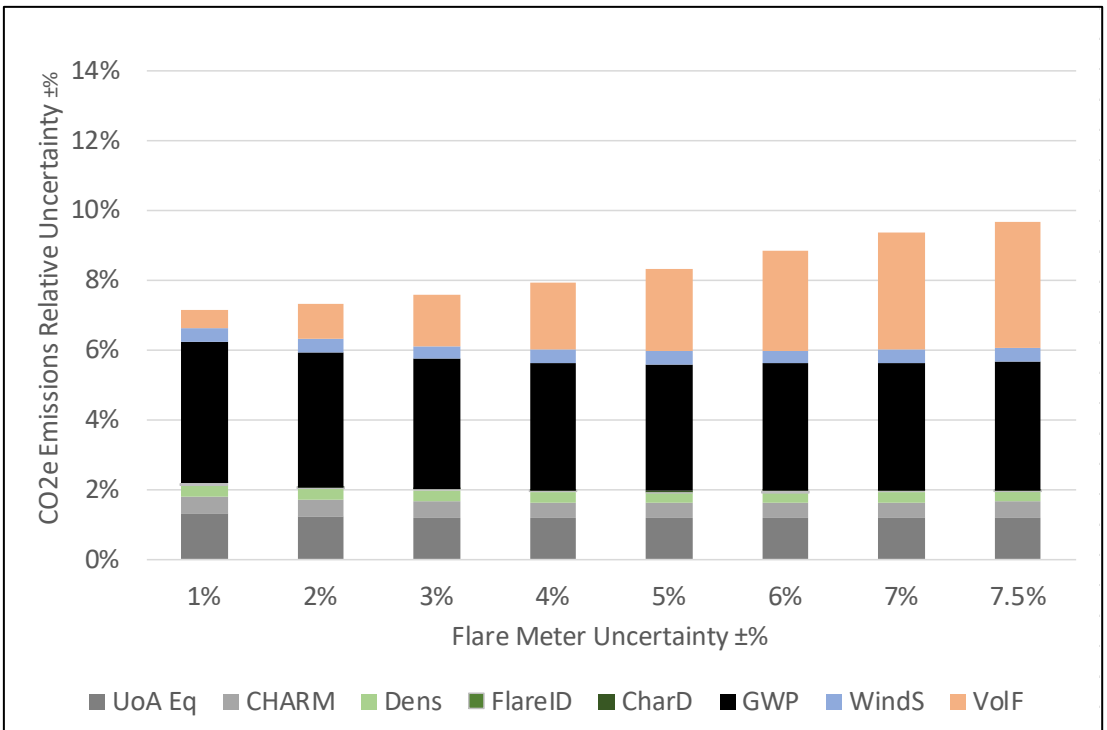

GWP	81.2		
CE	99.16%		
CO2e	0.314	kg/s	± 0.03 abs, kg/s, ± 9.6 % rel

Figure 18 CO2e Uncertainties, Flare Meter Uncertainty Sensitivity, GWP-20

Note that the y-axis scale has been held constant to allow the impacts on uncertainty between sensitivity cases to be more easily compared, though for the increased wind speed case the axis range had to be increased.

The GWP uncertainty increases the total CO2e uncertainty and becomes the most dominant contributor, limiting the impact reductions in flow meter uncertainty have on total CO2e emission uncertainties.

Including the GWP uncertainty in the CO2e uncertainty estimations, expresses our uncertainty in our estimate of the true CO2e emissions. However, it could be argued that the GWP value is a specified constant in the equation to report CO2e emissions and that there should be no uncertainty attached to its value. This would represent the uncertainty in the reported value as opposed to the uncertainty in our estimate of the true value.

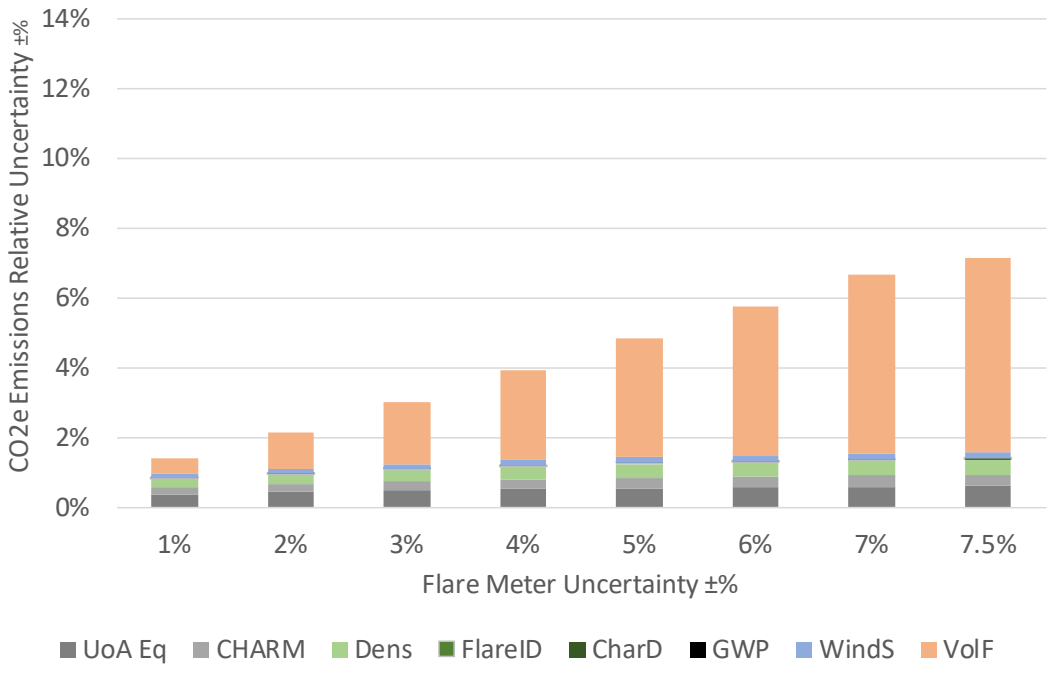

GWP	27.9		
CE	99.16%		
CO2e	0.278	kg/s	± 0.02 abs, kg/s, ± 7.1 % rel

Figure 19 CO2e Uncertainties, Flare Meter Uncertainty Sensitivity, No GWP Uncertainty

The benefits of improving flow meter uncertainty are more apparent.

The following charts show the impact of reducing LHV and increasing wind speed.

Reducing the LHV to 30 MJ/kg:

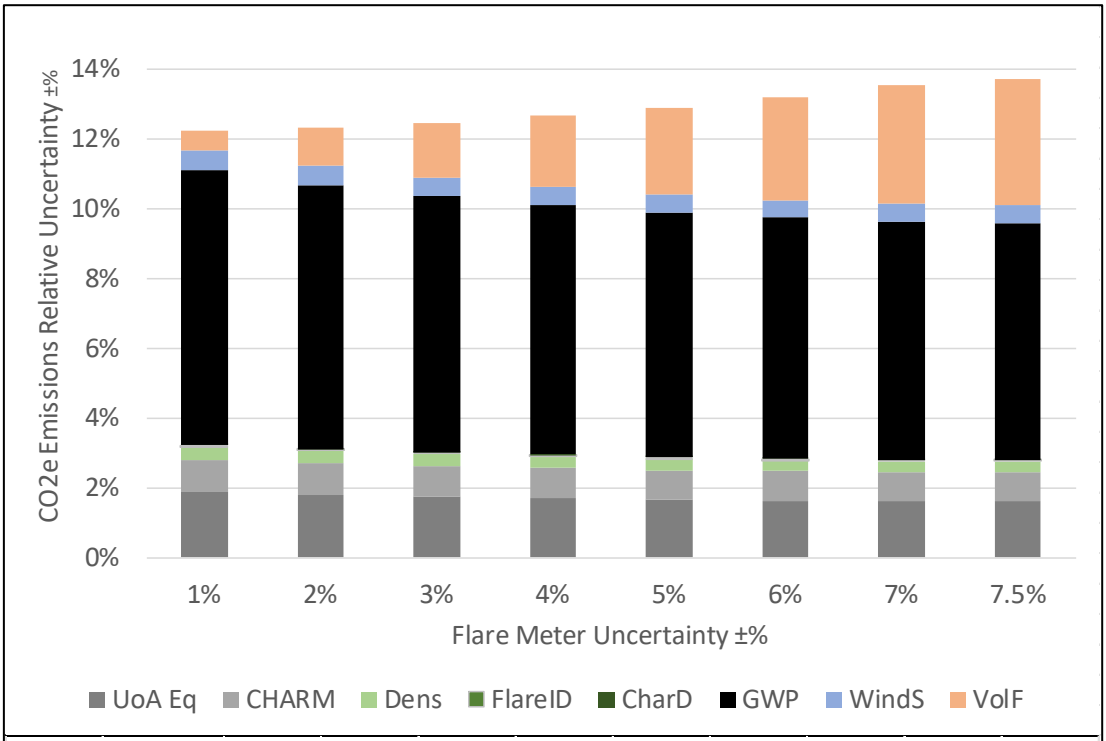

GWP	27.9		
CE	96.31%		
CO2e	0.334	kg/s	± 0.046 abs, kg/s, ± 13.7 % rel

Figure 20 CO2e Uncertainties, Flare Meter Uncertainty Sensitivity, LHV 30 MJ/kg

Increasing the wind speed to 25 m/s:

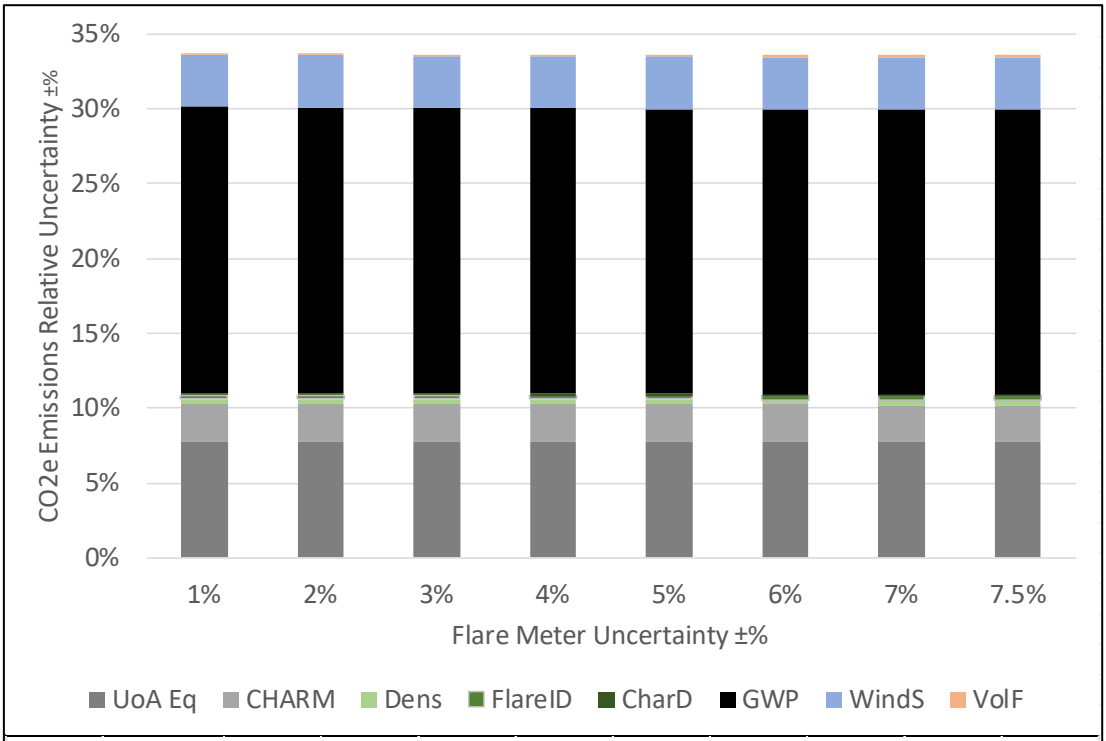

GWP	27.9		
CE	82.78%		
CO2e	0.6	kg/s	± 0.202 abs, kg/s, ± 33.6 % rel

Figure 21 CO2e Uncertainties, Flare Meter Uncertainty Sensitivity, Wind Speed 25 m/s

Not that the y-axis scale has been extended for this plot.

6 CONCLUSIONS

Wind tunnels are considered the best method of measuring combustion efficiency as they capture all the flare plume products and obtain samples representative of the complete combustion process.

The UoA have developed a methodology to measure combustion efficiency using a closed loop wind tunnel. The method exhibits uncertainties typically less than ±0.1% absolute at CE values above 90%. The CE measurements themselves therefore do not contribute significantly to the uncertainty associated with the fitted UoA equation.

Based on the measured CE data, the UoA development of a semi-empirical equation that calculates combustion efficiency as a function of two dimensionless groups (which are functions of fuel type, wind speed, flare jet exit velocity, flare stack outside diameter and the mass based LHV of the flare gas).

The uncertainty in the coefficients of the UoA equation along with a covariance term was determined based on the least squares regression of the data.

In operation the measurement or calculation of the flare LHV, exit velocity, flare diameter and wind speed introduce additional uncertainty into the calculated CE. The exit velocity, flare diameter and wind speed can be obtained from direct measurements and their uncertainties

determined using conventional methods. The LHV is more difficult to measure on a continuous basis.

The study demonstrated that the LHV of the flare gas can be reliably estimated using process simulation. This has been verified by comparing the results of Accord's CHARM simulation with sampled flare data from a North Sea platform. CHARM also allows the uncertainty in the LHV to be calculated, which for the case just mentioned was of the order ±0.6% in relative terms.

A parametric uncertainty analysis of the combustion efficiency illustrated:

- The importance of the covariance between the UoA coefficients
- The uncertainty in CE increases as CE itself decreases
- The CE increasing windspeed and decreasing LHV, flare exit velocity and flare diameter
- The exponential nature of the UoA equation, resulted in the CE uncertainty being log-normally distributed. The resulting asymmetry in CE uncertainty becomes more pronounced as combustion efficiency decreases.

A similar parametric analysis of the CO2e emissions rate revealed:

- At high CE values the flare flow rate is the most dominant contributor to the CO2e uncertainty and reducing the flow rate uncertainty has a direct impact on the CO2e uncertainty.
- The relatively high uncertainty in the methane GWP values from the IPCC reports means that the GWP is a significant contributor to the true CO2e emissions uncertainty.
- The choice of 100 year versus 20-year GWP has significant impacts on both the CO2e emission total and its uncertainty.
- There is also a question regarding whether the uncertainty in the reported CO2e emissions should include the GWP uncertainty.
- A fall in the CE as a result of reduced LHV or increased wind speed increases the CO2e uncertainty and reduces the benefit of reducing flare flow measurement uncertainty.

In conclusion, this study underscores the importance of rigorous uncertainty analysis in offshore flare combustion efficiency calculations. Based on the UoA equation as a foundational framework, we have improved our understanding of the complex interplay between input parameters, mathematical formulations, and measurement uncertainties.

Sensitivity analysis provides insights into the relative importance of different parameters and informs strategies for improving measurement accuracy and reliability.

Understanding and quantifying uncertainty are essential for making informed decisions and implementing effective mitigation strategies to minimize environmental impact.

7 NOTATION

A_f	Cross sectional area of the flare tip (m^2)
A	rate of change of hydrocarbon mole fraction divided by temperature ($K^{-1}s^{-1}$)
B	rate of change of CO_2 mole fraction divided by temperature ($K^{-1}s^{-1}$)
C	rate of change of CO mole fraction divided by temperature ($K^{-1}s^{-1}$)
d	flare outer diameter (m)
E_{CO2e}	mass of CO2 produced per mass of unburnt flare gas (kg/kg)
g	acceleration due to gravity (m/s^2)

GWP_{CH4}	GWP of methane (kg/kg)
LHV_{CH4}	mass based lower heating value methane (MJ/kg)
LHV_f	mass based lower heating value flare stream (MJ/kg)
m	carbon number
m_{CO2}	mass of CO2 in the tunnel (kg)
$\dot{m}_{CO2,Comb}$	mass flow of CO2 produced by combustion (kg/s)
$\dot{m}_{CO2,Inh}$	mass flow of CO2 inherent in the fuel gas (kg/s)
$\dot{m}_{CO2,Infil}$	mass flow of CO2 into the tunnel due to leakage (kg/s)
$\dot{m}_{CO2,Exfil}$	mass flow of CO2 out of the tunnel due to leakage (kg/s)
M_{CO2e}	total mass flow of CO_2 equivalent emitted by the flare (kg/s)
n	hydrogen number
Q_f	total volumetric flow of unburnt flare jet (m^3/s)
T	tunnel temperature (K)
t	time (s)
t'	end time (s)
U_w	wind speed (m/s)
U_f	flare jet exit speed (m/s)
Y_{HC}	mole fraction of hydrocarbons in the tunnel
Y_{CO}	mole fraction of carbon monoxide in the tunnel
Y_{CO_2}	mole fraction of carbon dioxide in the tunnel
$Y_{C_mH_n}$	mole fraction of hydrocarbons in the tunnel
α	coefficient of linear fit
β	coefficient of linear fit
μ	combustion efficiency
μ_{DRE}	destruction removal efficiency of methane

4 REFERENCES

[1] *Kostiuk L, Johnson M, Thomas G, University of Alberta Flare Research Project Final Report, November 1996 – September 2004, http://www.mece.ualberta.ca/groups/combustion/flare/papers/Final%20Report2004.pdf.*

[2] *OGMP Technical Guidance Document – Flare Efficiency, June 2021.*

[3] "Joint Committee for Guides in Metrology (JCGM), “Evaluation of Measurement Data – Supplement 1 to the ‘Guide to the Expression of Uncertainty in Measurement’ – Propagation of Distributions Using and Monte Carlo Method” JCGM 101: 2008, France 2008".

[4] "Peebles B, Stockton P, Offshore flares: measurement and calculation of combustion efficiency, methane and CO2e emissions, Global Flow Measurement Workshop, 25-27 October 2022".

[5] "Allen, D.T. and Torres, V.M. (2011). TCEQ 2010 Flare study final report (No. PGA No. 582-8-862-45-FY09-04). Texas Commission on Environmental Quality (TCEQ), Austin, TX.".

[6] "E. Bourguignon, M.R. Johnson, L.W. Kostiuk, The Use of a Closed-Loop Wind Tunnel for Measuring the Combustion Efficiency of Flames in a Cross Flow, COMBUSTION AND FLAME 119:319–334 (1999)".

[7] "Johnson MR and Kostiuk LW, Efficiencies of Low-Momentum Jet Diffusion Flames in Crosswinds, COMBUSTION AND FLAME 123:189–200 (2000)".

[8] "Johnson MR and Kostiuk LW, A Parametric Model for the Efficiency of Flare in a Crosswind Proceedings of the Combustion Institute, Volume 29, 2002/pp. 1943–1950".

[9] "WebPlotDigitizer," [Online]. Available: https://automeris.io/.

[10] "Guide to the Expression of Uncertainty in Measurement, International Organisation for Standardisation, ISO/IEC Guide 98:1995.".

[11] "Smith C, Nicholls ZRJ, et al. The Earth's Energy Budget, Climate Feedbacks, and Climate Sensitivity Supplementary Material. In Climate Change 2021: The Physical Science Basis.," The Physical Science Basis. Contribution of Working Group I to the Sixth Assessment Report of the Intergovernmental Panel on Climate Change. Available from https://www.ipcc.ch/..